Generation of Orthogonally Polarized Mode-Locked Lasers at Wavelength of 1342 nm
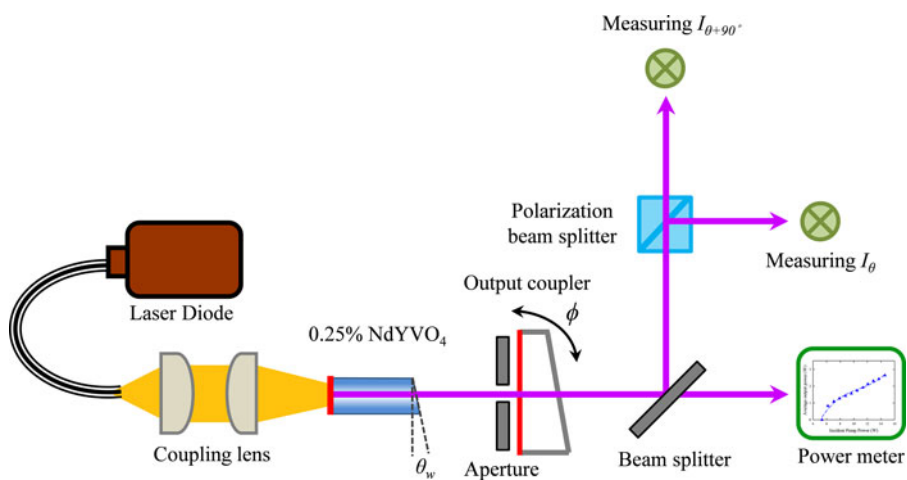
Hsing-Chih Liang
Feng-Lan Chang
Tai-Wei Wu
Cheng-Lin Sung
Yung-Fu Chen

Generation of Orthogonally Polarized Mode-Locked Lasers at Wavelength of 1342 nm

Hsing-Chih Liang,[1] **Feng-Lan Chang,**[2] **Tai-Wei Wu,**[2]
Cheng-Lin Sung,[2] **and Yung-Fu Chen**[2,3]

[1]Institute of Optoelectronic Science, National Taiwan Ocean University, Keelung 20224, Taiwan, R.O.C.
[2]Department of Electrophysics, National Chiao Tung University, Hsinchu 30010, Taiwan, R.O.C.
[3]Department of Electronics Engineering, National Chiao Tung University, Hsinchu 30010, Taiwan, R.O.C.

Abstract: A mode-locked laser with orthogonal polarization at the wavelength of 1342 nm is experimentally achieved by using the natural birefringence of the Nd:YVO$_4$ crystal. A total output power of 2.64 W could be obtained at an incident power of 14.4 W and the pulse durations are measured to be 15.1 and 16.9 ps with pulse repetition rates of 6.0 and 6.45 GHz for the laser output along the π- and σ-polarization, respectively. The mode-locked output is further found to exhibit a complex temporal trace with beat frequencies originated from the different central frequencies and pulse repetition rates.

Index Terms: Infrared lasers, diode-pumped lasers, solid state lasers, mode-locked lasers.

1. Introduction

Diode-Pumped solid-state lasers at 1.3 μm are attractive for many applications such as telecommunication, range finding, data storage, and scientific researches. Nowadays, Nd-doped gain media are widely used to efficiently generate 1.3-μm lasers at continuous-wave or pulsed operation [1]–[5]. For some applications, high-power passively mode-locked lasers at wavelength of 1.3 μm are prerequisite [6]. Among various pulsed lasers, Kerr-lens mode locking has been identified as a simple and practical technique to generate ultrafast pulses. The physical mechanism is comprehended to be associated with the self-focusing of laser beam and the amplitude modulation produced by either a hard aperture or a soft gain aperture [7]–[9]. Various experimental results reveal that a short cavity round-trip time and high Kerr nonlinearity can beneficially achieve the mode-locked operation [10]–[12]. By employing Nd-doped vanadate crystals with the large Kerr nonlinearities, diode-pumped self-mode-locked (SML) lasers at 1.3 μm have been demonstrated in short cavities with a linear polarization output [13], [14].

In addition to linearly polarized mode-locked lasers, orthogonally polarized dual-wavelength mode-locked lasers [15]–[20] have aroused considerable attention for various applications including
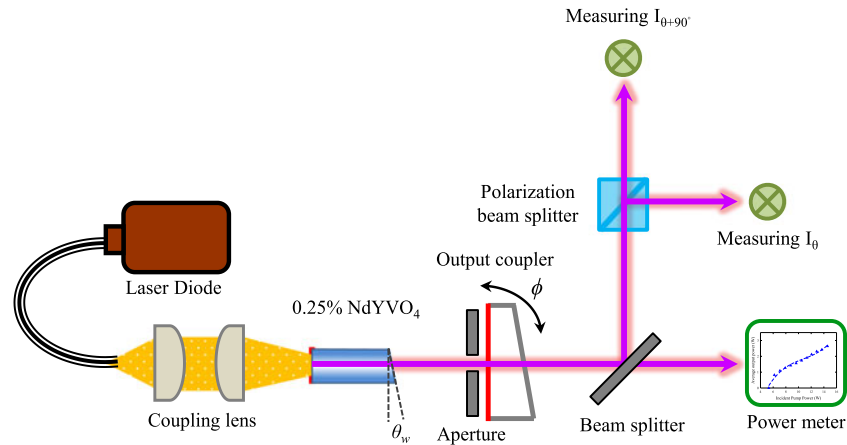
Fig. 1. Experimental setup for the orthogonally polarized self-mode-locked Nd:YVO$_4$ lasers at 1342 nm.

laser spectroscopy [21], asynchronous optical sampling [22], magnetization metrology controlling [23], and secure communication [24]. It has been reported that the orthogonal polarization output can be achieved in a single cavity with an identical repetition rates (synchronous) or different repetition rates (asynchronous) by exploiting the isotropic or anisotropic gain crystal, respectively. With a synchronous scheme, the tiny birefringence induced by the thermal stress in the gain medium can lead to laser emission with orthogonal polarized states [25]–[27]. Alternatively, with an asynchronous scheme, orthogonally polarized lasers can be realized by either using a birefringent crystal as the gain medium or inserting a birefringent element into the cavity [28], [29]. Since the vector mode-locked light sources show great potentials for extensive applications, it is desirable to develop orthogonally polarized SML lasers at 1.3 um.

In this work, we have explored the temporal dynamics of an asynchronously mode-locked laser with orthogonally polarized states. By utilizing the natural birefringence of a wedged Nd:YVO$_4$ gain crystal, the simultaneously SML laser at 1.34 μm with orthogonal polarization output was successfully achieved for the first time. Since the optical paths for the two orthogonally-polarized states are slightly different inside the resonator, the output polarization component can be easily manipulated by precisely tuning the orientation of the output coupler [30]. More importantly, the experimental result reveals that there exists a specific tilted angle of the output coupler for achieving a stable orthogonally-polarized SML output with balanced intensities for each polarized state. Under the optimal condition for the balanced orthogonal-polarization intensities, the total average output power of 2.64 W can be obtained with an incident pump power of 14.4 W. The pulse durations are measured to be 15.1 ps and 16.9 ps with repetition rates of 6.0 GHz and 6.45 GHz for the output beam along the π- and σ-polarizations, respectively. It is also found that the SML output composed of two orthogonal polarization components displays a complex beating modulation in temporal traces. We have also theoretical reconstructed the complex pulse train in an asynchronous mode-locked laser different central frequencies.

2. Experimental Setup

A schematic diagram of the laser experiment is shown in Fig. 1. The cavity configuration is a simple flat-flat resonator. The active medium is an *a*-cut 0.25 at.% Nd:YVO$_4$ crystal with dimensions of $3 \times 3 \times 8$ mm^3 and the *c* axis (π axis) of crystal was arranged to be along the *x* axis. One facet of the laser crystal was normal to the crystal axis and was high-reflection coated at 1342 nm (>99.8%) and high transmission coated at 808 nm. The second facet was antireflection coated at 1342 nm and wedged 0.5° to eliminate the Fabry-Perot etalon effect. The cavity length, L_{cav}, was initially designed to be 15.6 mm. With the refractive indices of $n_\pi = 2.154$ and $n_\sigma = 1.949$, the optical path length was set to be approximately 25.15 mm and 23.1 mm for π- and σ-polarizations,
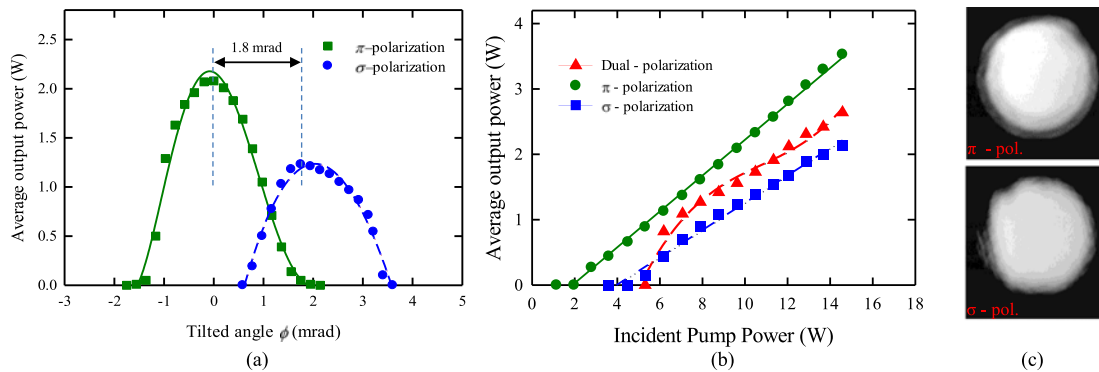
Fig. 2. (a) Dependence of output performance of two orthogonal polarization states on the tilted angle of OC. (b) Average output power versus the incident pump power for σ- and π-polarized optimization and balanced orthogonal-polarization intensities. (c) Polarization-resolved output beam profiles of the two orthogonal emissions.

respectively. The laser crystal was wrapped with indium foil and mounted in a water-cooled cooper holder. The water temperature was maintained at 16 °C to ensure stable laser output. A wedged flat mirror with 7% transmission at 1342 nm and high transmission at 1064 nm was used as an output coupler. In order to suppress the excitation of high-order transverse modes, a physical aperture with aperture radius of 175 μm was inserted into the cavity. The pump source was a 16-W, 808-nm fiber-coupled laser diode with a core diameter of 400 μm and a numerical aperture of 0.22. A focusing lens with 25-mm focal length and 90% coupling efficiency was used to reimage the pump beam into the laser crystal. The average pump diameter was approximately 220 μm.

3. Experimental Results and Discussions

First of all, we explore the dependence of output performance with respect to π- and σ-polarization emissions in the Nd:YVO$_4$ laser on the orientation of the output coupler. As shown in Fig. 2(a), the output polarization state can be easily controlled by precisely tilting the orientation of output coupler. Note that the tilting angle ϕ is defined as the included angle with respect to the orientation of output coupler corresponding to the maximum output power at π-polarization. At the pumped power $P_{\text{in}} = 10.5$ W, the angular separation θ_{spe} between the π- and σ-polarization under the individual maximum output power is found to be 1.8 mrad, as shown in Fig. 2(a). The intrinsic angular separation for the two orthogonal polarizations mainly results from the different refractive indices at 1342 nm for the a-cut Nd:YVO$_4$ crystal with $n_\pi = 2.154$ and $n_\sigma = 1.949$ which corresponding to different optical axes for the wedged crystal. With the Snell's law under the small-angle approximation, we can theoretically derive the angular separation to be $\theta_{spe} = (n_\pi - n_\sigma)\theta_w \sim 1.79$ mrad which is in a good agreement with the experimental results. The output power with respect to incident power for the σ- and π-polarizations of the laser system is indicated in Fig. 2(b). The pump threshold is around 4.5 and 2.0 W, and the maximum average output power is found to reach 2.13 and 3.53 W under the pump power of 14.4 W for the σ- and π-polarizations, respectively. More importantly, by precisely controlling the tilting angle, the laser can operate under balanced orthogonal-polarization intensities. Fig. 2(b) shows experimental results for the average output power of the SML NdYVO$_4$ laser versus incident pump power under balanced orthogonal-polarization intensities, corresponding to the tilted angle $\phi = 1.17$ mrad. At a pump power of 14.4 W, the maximum output power of 2.64 W can be achieved, as shown in Fig. 2(b). Due to the contribution of both σ- and π-polarizations, the average output power under balanced orthogonal-polarization operation is even higher than σ-polarization output emission. It is believed that this configuration is not only simple but also high efficient. Although the two orthogonal polarizations were to be emitted in different directions, the beam profiles still can be seen well-superimposed over a fine distance behind the output coupler.
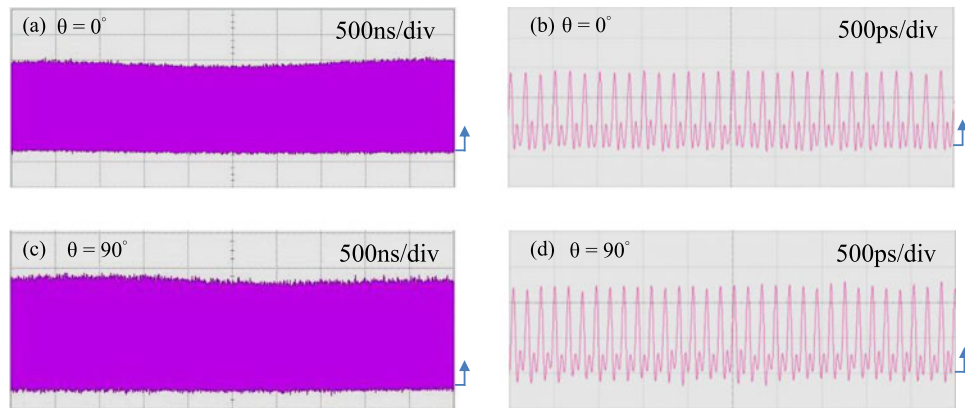
Fig. 3. Polarization-resolved output intensity I_{0° (t) with the time span of: (a) 5 μs and (b) 5 ns; polarization-resolved output intensity I_{90° (t) with the time span of: (a) 5 μs and (b) 5 ns.

The polarization-resolved output beam profiles of the two orthogonal output were experimentally observed to be well-superimposed at the position of 100 mm behind the output coupler and the lasing modes are near TEM$_{00}$ fundamental mode with the beam quality better than 1.3 under dual-polarized operation, as shown in Fig. 2(c).

The temporal dynamics was detected by a high-speed InGaAs photodetector (Electro-optics Technology Inc. ET-3500 with rise time of 35 ps), whose output signal was connected to a digital oscilloscope (Agilent DSO 80000) with a 10 GHz electrical bandwidth and a sampling interval of 25 ps. For the sake of description, the direction of π- and σ-polarization emissions are denoted as the x- and y-axes. Fig. 3 shows the polarization-resolved output intensities I_θ(t) at $\theta = 0^\circ$ and $\theta = 90^\circ$ with two different timescales under balanced orthogonal-polarization intensities at the pumped power $P_{in} = 10.5$ W, where θ is the analyzer angle with respect to the x axis. It can be seen that the time traces exhibit a full modulation and complete mode-locking is achieved in both I_{0°(t) and I_{90°(t), as observed in our previous work [13], [14]. The pulse repetition rates of π-polarization emission and σ-polarization emission were found to be 6.0 GHz and 6.45 GHz which are consistent with the optical path lengths, respectively.

The optical spectrum of laser output was recorded with a Michelson optical interferometer (Advantest, Q8347) with a resolution 0.003 nm that is also able to perform optical spectral analysis by Fourier transformation of the first-order field autocorrelation. Fig. 4 depicts the lasing spectrum and autocorrelation trace for the two orthogonally polarized states at an incident power of 10.5 W. It can be seen that the central wavelengths for the two polarization states are observed to be nearly at 1342.15 nm with tiny difference was 0.012 nm corresponding to a central frequency difference of 1.7 GHz. The full width at half maximum (FWHM) values of the lasing spectra at π- and σ-polarization states are 0.18 nm and 0.16 nm, respectively. The longitudinal mode spacings within each spectral band are found to be 0.036 nm and 0.039 nm that are consistent with the pulse repetition rates of 6.0 GHz (π-polarization) and 6.45 GHz (σ-polarization). A commercial autocorrelator (APE Pulse Check, Angewandte Physik and Elektronik GmbH) was employed to measure the mode-locked pulses. Fig. 4(c) and (d) show the autocorrelation traces of the single pulse for two orthogonally polarized emissions. Assuming the Gaussian-shape temporal profile, the pulse widths were evaluated to be 15.1 ps for π-polarization and 16.9 ps for σ-polarization. Although the optical spectra have a slight asymmetry, the experimental results of digital oscilloscope and autocorrelation traces are revealed that the mode-locking are clean. As a result, the time-bandwidth products of the mode-locked pulses were estimated to be 0.453 and 0.45, respectively. Both values are slightly greater than the Fourier-limit value of 0.441 which indicates there exist little frequency chirps in the present pulses. Even though the polarization-resolved output intensities for $\theta = 0^\circ$ and $\theta = 90^\circ$ display the temporal feature of a conventional mode-locked laser, the pulse train of the polarization-
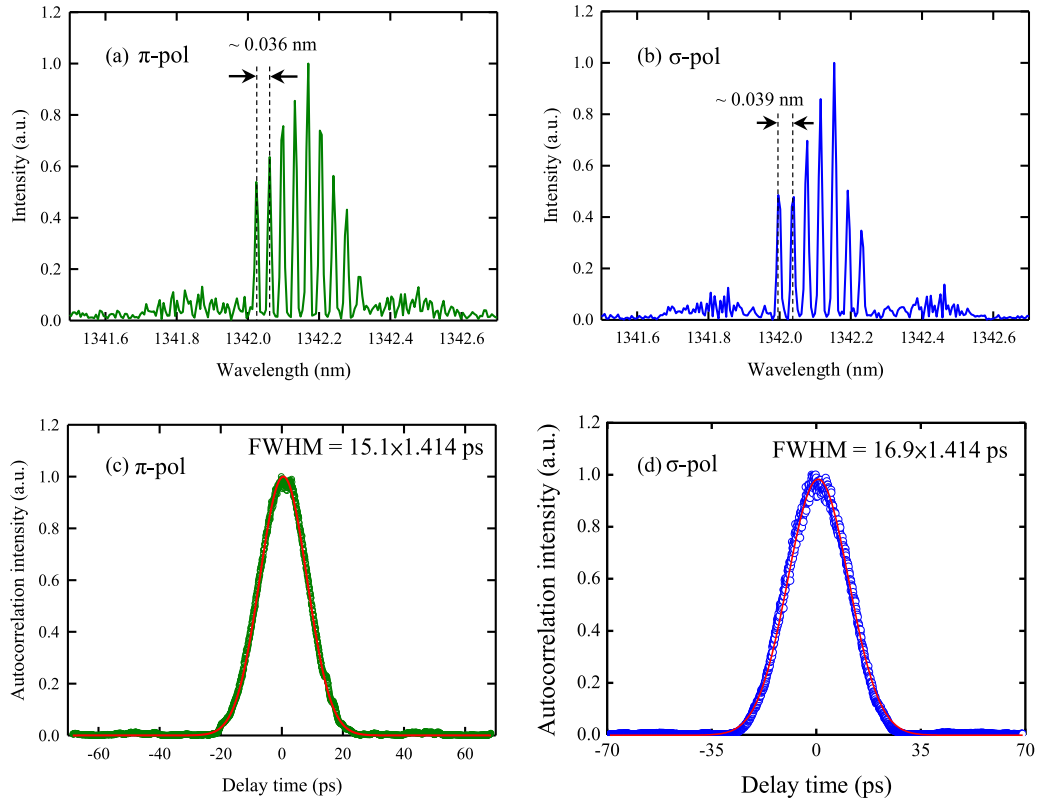
Fig. 4. Experimental optical spectrum of the orthogonally polarized Nd:YVO$_4$ lasers (a) π-polarization; (b) σ-polarization; Autocorrelation traces of the output pulses (c) π-polarization; (d) σ-polarization.

resolved intensity along $\theta = 45°$ is observed to exhibit a complex temporal dynamics, as shown in Fig. 5(a) and (b) with two timescales. In order to elucidate the complex temporal profiles more quantitatively, we numerically reconstructed the complex temporal traces. The normalized complex electric field for mode-locked laser form by N longitudinal modes can be expressed as:

$$E(t) = \frac{1}{N} e^{j2\pi f_0 t} \, e^{-i\pi(N+1)f_{\mathrm{rep}}t} \sum_{n=1}^{N} e^{j2\pi n f_{\mathrm{rep}}t} = e^{j2\pi f_0 t} \frac{\sin(N\pi f_{\mathrm{rep}}t)}{N \sin(\pi f_{\mathrm{rep}}t)} \tag{1}$$

where f_0 is the central frequency and f_{rep} is the longitudinal mode spacing. Considering the optical axis for light propagation is along z-direction, the polarization state of the mode-locked laser can be described as the vector sum of the x-(horizontal) and y-(vertical) components along the principal axes. For the in-phase and asynchronous two orthogonally polarized mode-locked laser, the polarization-resolved output intensity is then given by

$$I(t) = \left| \cos(\theta)E_x(t) + \sin(\theta)E_y(\theta) \right|^2 \tag{2}$$

$$E_j(t) = e^{j2\pi f_{0,j}t} \frac{\sin(N_j\pi f_{\mathrm{rep},j}t)}{N_j \sin(\pi f_{\mathrm{rep},j}t)}, \quad j = x, y \tag{3}$$

Substituting the experimental parameters with $f_{\mathrm{rep},x} = 6.0\,\mathrm{GHz}$, $f_{\mathrm{rep},y} = 6.5\,\mathrm{GHz}$, $\Delta f_0 = 1.7\,\mathrm{GHz}$, $N_x = 8$, and $N_y = 7$ into Eq. (2) and Eq. (3), the complex pulse train could be numerically reconstruct, as shown in Fig. 5(c) and (d). It can been seen that numerical calculations agree very well with the experimental results. The excellent consistency between the experimental and numerical results validates that the present analysis can well describe the complex temporal traces observed
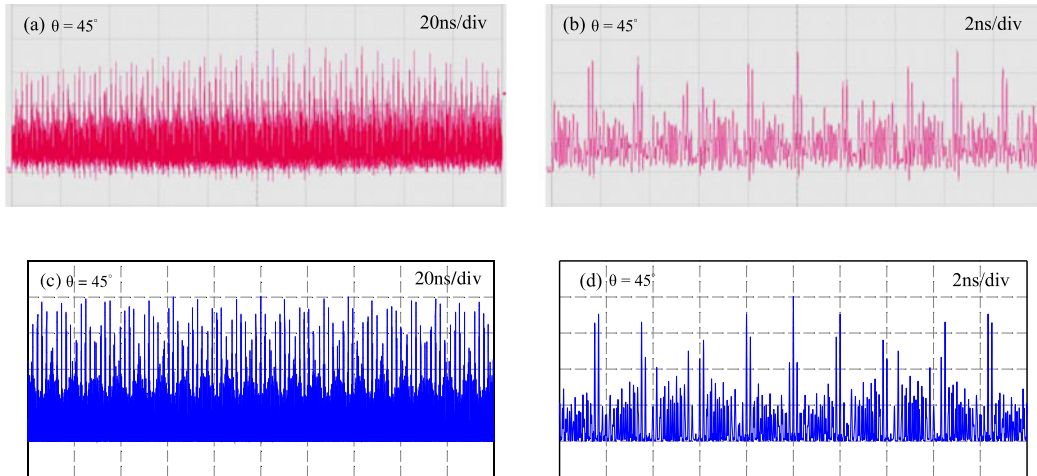
Fig. 5. Experimental polarization-resolved output intensity $I_{45°}$ (t) with the time span of: (a) 200 ns and (b) 20 ns; Numerical reconstructed polarization-resolved output intensity $I_{45°}$ (t) with the time span of: (a) 200 ns and (b) 20 ns.
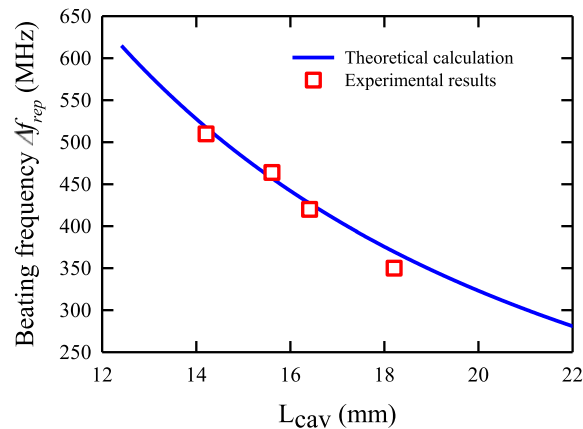

Fig. 6. Beat frequency of orthogonally polarized Nd:YVO$_4$ laser as a function of the geometric length of cavity.

in an asynchronous mode-locked laser with two orthogonally polarized states corresponding to different central frequencies and pulse repetition rates. Note that the complex temporal traces can be improved with fine-tuning of the cavity length to reduce the difference in central frequencies. Furthermore, the difference in the pulse repetition rates between two orthogonally polarized pulse trains can be calculated to be $\Delta f_{rep} = f_{rep,y} - f_{rep,x} = \Delta n L_{cry}(c/2L_{cav}^2)$, where L_{cav} is the geometric length of the cavity, Δn and L_{cry} are the natural birefringence and length of gain crystal. It can be clearly seen that difference of repetition rate can be tuning by adjusting the geometric length of cavity. Fig. 6 shows both experimental and calculated results for the beat frequency versus the geometric length of cavity. Consequently, the repetition rate difference Δf_{rep} can be approximately in the range of 500–350 MHz for the geometric length of cavity within 14–18 mm.

4. Conclusion

In conclusion, we have experimentally realized an asynchronous self-mode-locking of two orthogonally polarized emissions in a Nd:YVO$_4$ laser at the wavelength of 1342 nm by exploiting the natural

birefringence of the gain medium. At an incident power of 14.4 W, the total output power of 2.64 W could be obtained for the two polarized states with balanced output intensities. For each orthogonally polarized mode-locked components, the pulse durations and the pulse repetition rates are measured to be 15.1 (16.9) ps and 6.0 (6.45) GHz for the laser output along the π- (σ-) polarization, respectively. Furthermore, the complex pulse train with temporal beats between two orthogonally polarized states have been observed and numerically reconstructed. The excellent consistency between the experimental and numerical results confirmed that the origin of complex beating modulation was not only pulse repetition rates difference but also central frequencies difference. We believe that this work can offer a simple method for generating orthogonally polarized mode-locked lasers for further applications.

References

[1] A. Di Lieto, P. Minguzzi, A. Pirastu, S. Sanguinetti, and V. Magni, "A 7-W diode-pumped NdYVO$_4$ cw laser at 1.34 μm," *Appl. Phys. B*, vol. 75, no. 4, pp. 463–466, Oct. 2002.

[2] X. F. Zhang, F. Q. Li, N. Zong, X. Y. Le, D. F. Cui, and Z. Y. Xu, "37 W 888-nm-pumped grown-together composite crystal YVO$_4$/Nd:YVO$_4$/ YVO$_4$ oscillator at 1342 nm," *Laser Phys.*, vol. 21, no. 8, pp. 1393–1397, Jul. 2011.

[3] N. Pavel, T. Dascalu, N. Vasile, and V. Lupei, "Efficient 1.34-μm laser emission of Nd-doped vanadates under in-band pumping with diode lasers," *Laser Phys. Lett.*, vol. 6, no. 1, pp. 38–43, Sep. 2009.

[4] H. T. Huang *et al.*, "Diode-pumped passively Q-switched Nd:Gd$_{0.5}$Y$_{0.5}$VO$_4$ laser at 1.34 μm with V^{3+}:YAG as the saturable absorber," *Opt. Exp.*, vol. 17, no. 9, pp. 6946–6951, Apr. 2009.

[5] K. Liu *et al.*, "High peak power 4.7 ns electro-optic cavity dumped TEM00 1342-nm Nd:YVO$_4$ laser," *Appl. Opt.*, vol. 54, no. 4, pp. 717–720, Jan. 2015.

[6] R. Moncorgé *et al.*, "Nd doped crystals for medical laser applications," *Opt. Mater.*, vol. 8, no. 1, pp. 109–119, Apr. 1997.

[7] G. Q. Xie, D. Y. Tang, L. M. Zhao, L. J. Qian, and K. Ueda, "High-power self-mode-locked Yb:Y$_2$O$_3$ ceramic laser," *Opt. Lett.*, vol. 32, no. 18, pp. 2741–2743, Sep. 2007.

[8] A. A. Lagatsky, C. T. A. Brown, and W. Sibbett, "Highly efficient and low threshold diode-pumped Kerr-lens mode-locked Yb:KYW laser," *Opt. Exp.*, vol. 12, no. 17, pp. 3928–3933, Aug. 2004.

[9] H. C. Liang, H. L. Chang, W. C. Huang, K. W. Su, Y. F. Chen, and Y. T. Chen, "Self-mode-locked Nd:GdVO$_4$ laser with multi-GHz oscillations: Manifestation of third-order nonlinearity," *Appl. Phys. B*, vol. 97, no. 2, pp. 451–455, May 2009.

[10] F. Krausz, T. Brabec, and C. Spielmann, "Self-starting passive mode locking," *Opt. Lett.*, vol. 16, no. 4, pp. 235–237, Feb. 1991.

[11] W. Z. Zhuang, M. T. Chang, H. C. Liang, and Y. F. Chen, "High-power high-repetition-rate subpicosecond monolithic Yb:KGW laser with self-mode locking," *Opt. Lett.*, vol. 38, no. 14, pp. 2596–2599, Jul. 2013.

[12] C. Y. Lee, C. C. Chang, H. C. Liang, and Y. F. Chen, "Frequency comb expansion in a monolithic self-mode-locked laser concurrent with stimulated Raman scattering," *Laser Photon. Rev.*, vol. 8, no. 5, pp. 750–755, May 2014.

[13] H. C. Liang, Y. J. Huang, W. C. Huang, K. W. Su, and Y. F. Chen, "High-power, diode-end-pumped, multigigahertz self-mode-locked Nd:YVO$_4$ laser at 1342 nm," *Opt. Lett.*, vol. 35, no. 1, pp. 4–6, Jan. 2010.

[14] T. W. Wu, C. H. Tsou, C. Y. Tang, H. C. Liang, and Y. F. Chen, "A high-power harmonically self-mode-locked Nd:YVO$_4$ 1.34-μm laser with repetition rate up to 32.1 GHz," *Laser Phys.*, vol. 24, Mar. 2014, Art. no. 045803.

[15] Q. Yang *et al.*, "Dual-wavelength mode-locked Yb:LuYSiO$_5$ laser with a double-walled carbon nanotube saturable absorber," *Laser Phys. Lett.*, vol. 9, no. 2, pp. 135–140, Dec. 2012.

[16] S. T. Cundiff, B. C. Collings, N. N. Akhmediev, J. M. Soto-Crespo, K. Bergman, and W. H. Knox, "Observation of polarization-locked vector solitons in an optical fiber," *Phys. Rev. Lett.*, vol. 82, no. 20, pp. 3988–3991, May 1999.

[17] L. M. Zhao, D. Y. Tang, H. Zhang, and X. Wu, "Polarization rotation locking of vector solitons in a fiber ring laser," *Opt. Exp.*, vol. 16, no. 14, pp. 10053–10058, Jul. 2008.

[18] S. V. Sergeyev, C. Mou, A. Rozhin, and S. K. Turitsyn, "Vector solitons with locked and processing states of polarization," *Opt. Exp.*, vol. 20, no. 24, pp. 27434–274400, Nov. 2012.

[19] J. Thévenin, M. Vallet, and M. Brunel, "Dual-polarization mode-locked Nd:YAG laser," *Opt. Lett.*, vol. 37, no. 14, pp. 2859–2861, Jul. 2012.

[20] J. Javaloyes, J. Mulet, and S. Balle, "Passive mode locking of lasers by crossed-polarization gain medium," *Phys. Rev. Lett.*, vol. 97, Oct. 2006, Art. no. 163902.

[21] B. Bernhardt *et al.*, "Cavity-enhanced dual-comb spectroscopy," *Nature Photon.*, vol. 4, no. 1, pp. 55–57, Jan. 2010.

[22] A. Bartels *et al.*, "Ultrafast time-domain spectroscopy based on high-speed asynchronous optical sampling," *Rev. Sci. Instrum.*, vol. 78, Feb. 2007, Art. no. 035107.

[23] N. Kanda, T. Higuchi, H. Shimizu, K. Konishi, K. Yoshioka, and M. Kuwata-Gonokami, "The vectorial control of magnetization by light," *Nature Commun.*, vol. 2, Jun. 2011, Art. no. 362.

[24] G. D. VanWiggeren and R. Roy, "Communication with dynamically fluctuating states of light polarization," *Phys. Rev. Lett.*, vol. 88, Feb. 2002, Art. no. 097903.

[25] C. W. Xu, D. Y. Tang, H. Y. Zhu, and J. Zhang, "Mode locking of Yb:GdYAG ceramic lasers with an isotropic cavity," *Laser Phys. Lett.*, vol. 10, Aug. 2013, Art. no. 095702.

[26] C. L. Sung, H. P. Cheng, C. Y. Lee, C. Y. Cho, H. C. Liang, and Y. F. Chen, "Generation of orthogonally polarized self-mode-locked Nd:YAG lasers with tunable beat frequencies from the thermally induced birefringence," *Opt. Lett.*, vol. 41, no. 8, pp. 1781–1784, Apr. 2016.

[27] H. P. Cheng, T. L. Huang, C. Y. Lee, C. L. Sung, C. Y. Cho, and Y. F. Chen, "Monolithic dual-polarization self-mode-locked Nd:YAG 946-nm lasers: Controlling beating frequency and observation of temporal chaos," *Opt. Exp.*, vol. 24, no. 21, pp. 23829–23837, Oct. 2016.

[28] S. M. Link *et al.*, "Dual-comb modelocked laser," *Opt. Exp.*, vol. 23, no. 5, pp. 5521–5531, Mar. 2015.

[29] S. M. Link, M. Mangold, M. Golling, A. Klenner, and U. Keller, "Gigahertz dual-comb modelocked diode-pumped semiconductor and solid-state lasers," *Proc. SPIE*, vol. 9734, Mar. 2016, Art. no. 973406.

[30] A. Agnesi and S. Dell' Acqua, "High-peak-power diode-pumped passively Q-switched Nd:YVO$_4$ laser," *Appl. Phys. B*, vol. 76, no. 4, pp. 351–354, Mar. 2003.